# Gastric tumorigenesis induced either by *Helicobacter pylori* infection or chronic alcohol consumption through IL-10 inhibition

**Faisal Aziz**
University of Minnesota Hormel Institute
**Abhijit Chakarobaty**
University of Minnesota Hormel Institute
**Kandong Liu**
Zhengzhou University
**Hisae Yoshitomi**
University of Minnesota Hormel Institute
**Xiang Li**
Zhengzhou University
**Josh Monts**
University of Minnesota Hormel Institute
**Gang Xu**
Zhengzhou University
**Yonghan Li**
Zhengzhou University
**Ruihua Bai**
Zhengzhou University
**Ann M. Bode**
University of Minnesota Hormel Institute
**Zigang Dong** ( zgdong@hci-cn.org )
University of Minnesota Hormel Institute https://orcid.org/0000-0002-1076-0287

**Research**

**Keywords:** Helicobacter pylori (H. pylori), alcohol consumption, CD8, gastric tumorigenesis, interleukin-10 (IL-10), interleukin-1 (IL-1β)

**Posted Date:** February 10th, 2020

**DOI:** https://doi.org/10.21203/rs.2.23065/v1

# Abstract

Background Alcohol is class 1 carcinogen and results in 3.3 million deaths every year. H. pylori is also an important factor for gastric carcinogen. Alcohol consumption is emerging as an important contributor to gastric cancer, but there is no direct or experimental evidence of alcohol and H. pylori infection produce gastric cancer in human and animal model alone. Here, we provide insight into the molecular mechanisms driving gastric carcinogenesis.

Results Alcohol consumption, together with H. pylori infection, causes gastric cancer; interleukin-10 (IL-10) downregulation and mitochondrial metabolic dysfunction in CD8+ cells are also involved. IL-10 knockout accelerates tumor development in mice with either H. pylori infection or alcohol induced gastric cancer or both. IL-10 downregulation and CD-8+ cell dysfunction stimulates IL-1β secretion. Specifically, we show IL-10 inhibits glucose uptake and glycolysis and promotes oxidative phosphorylation with lactate inhibition. Consequently, In the absence of IL-10 signaling, CD8+ cells accumulate damaged mitochondria in a mouse model of gastric cancer induced with the combination of alcohol plus H. pylori infection, and this results in mitochondrial dysfunction and production of IL-1 β. IL-1β promotes H. pylori infection and reduces NKX6.3 gene expression, resulting in increased cancer cell survival and proliferation.

Conclusions Overall, the molecular mechanisms of gastric carcinogenesis include IL-10 inhibition resulting in lowered host immunity via mitochondrial dysfunction of CD8+ lymphocytes; gastric inflammation due to H. pylori infection, alcohol intake, and IL-1β production; and disruption of gastric-specific tumor suppressor NKX6.3 expression, which increases cancer cell survival and proliferation.


# 1. Introduction

*Helicobacter pylori* (*H. pylori)* is a Gram-negative bacterium that colonizes the stomach. The motility and helix- or spiral-shaped of *H. pylori* are well-adapted to the viscous environment of gastric mucus. As a result, this bacterium can burrow into the stomach's mucus layer, which is less acidic than the lumen[1]. Urease secretion, and the subsequent conversion of urea to ammonia, further improves microenvironment hospitability by neutralizing stomach acids. Other bacterial virulence factors interfere with host immune responses, plus, once *H. pylori* penetrates the stomach lining, gastric mucus offers protection against killing by immune cells. Overall, these characteristics help *H. pylori* to survive and colonize the harsh, acidic environment of the stomach[2,3,4].

The Centers for Disease Control and Prevention (CDC) estimates that roughly two-thirds of adults harbor *H. pylori.* Infection rates are even higher in countries like China and Japan. Without treatment, *H. pylori* infection is a major risk factor for gastrointestinal illnesses like chronic gastritis, peptic ulcers, and stomach cancer[5]. *H. pylori* was first classified as a carcinogen by the International Agency for Research on Cancer in 1994. In 2001, an epidemiologic study demonstrated that patients infected with *H. pylori* were nearly six times more likely to develop gastric cancer compared to uninfected people[6]. Since then,

the idea that *H. pylori* infection causes gastric cancer has gained acceptance; however, its mechanism for carcinogenesis is unknown.

Gastric cancer is associated with several known risk factors, including gender, age, and geography. Worldwide, gastric cancer is prevalent in China, Japan, and Southern and Eastern Europe; its incidence is less common in North America and in Northern and Western Africa[7]. In addition to *H. pylori* infection, diet and alcohol consumption are among the most widely accepted lifestyle risk factors, but the etiology of gastric cancer has not been fully elucidated[8,9]. Studies propose that alcohol may increase the risk of cancer by generating reactive oxygen species or by impairing the body's ability to absorb essential nutrients. Regardless, there is no consensus on alcohol consumption as a causative factor for gastric carcinogenesis[10]. Additionally, alcohol as an independent risk factor for gastric cancer has not been fully supported by direct experimental outcomes[11].

Lastly, host immune response plays a role in both *H. pylori* infection and gastric carcinogenesis. In particular, the anti-inflammatory cytokine interleukin–10 (IL–10) plays a key role in gastric inflammation. During infection, IL–10 inhibits the activity of Th1 cells, NK cells, and macrophages; these cell types are required for pathogen clearance, though they contribute to tissue damage as well. As a result, IL–10 levels must be tightly controlled to balance pathogen clearance with amelioration of immunopathology[12,13]. Regardless, IL–10 is a key immunoregulator produced by activated immune cells during infection[14]. Understanding how IL–10 controls inflammatory responses is necessary for understanding pathology driven by inflammation, such as gastric tumorigenesis.

Here, we explore the combined effect of *H. pylori* infection and alcohol consumption on the development of gastritis and later gastric cancer through IL–10 inhibition. Before now, no experimental animal models were used to study this association. To address this, we developed a novel mouse model that combined *H. pylori* infection and alcohol consumption to investigate the molecular mechanisms of gastric carcinogenesis.

# 2. Results

### 2.1. Alcohol consumption and *H. pylori* infection induce gastritis leading to gastric cancer

To investigate the role of alcohol consumption in the progression of *H. pylori*-associated gastric cancer, we developed a mouse model treated with a combination of alcohol and *H. pylori* infection to induce gastritis, leading to gastric cancer (Fig. 1a). Macroscopic morphometric analysis revealed that alcohol consumption induced gastric inflammation (at 32 weeks) as the initiating process, which led to tumor development (at 40 weeks) in the stomach of mice with *H. pylori* infection (Fig. 1b). Macroscopic analysis of tumor area revealed development of tumors only in mice treated with both *H. pylori* and alcohol ($52.88 \pm 9.085\ mm^2$; $p < 0.001$; $f = 33.88$; Fig. 1c). Solid tumor growth in mice treated with both alcohol and *H. pylori* confirmed the combinational role of alcohol and *H. pylori* in gastric tumorigenesis (Fig. 1c). Overall, these results indicated that *H. pylori* and alcohol together caused a progressive shift

from gastritis to gastric cancer. These results provided experimental animal evidence showing the combined effect of alcohol and *H. pylori* infection on the development of gastric cancer.

Histological analysis also showed multifocal elongation of the gastric pits, glandular atrophy, and a significant reduction in the glandular zone in atrophic foci. These changes were significantly less in mice treated with alcohol and infected with *H. pylori* exhibiting tumors, compared to mice treated with alcohol only (2.20 ± 0.2) or infected with *H. pylori* only (1.6 ± 0.245; $p < 0.001$; f = 27.50; Supplementary Fig. 1a-d). Dual treatment resulted in reduction of parietal cell components, especially parietal and chief cells, which were replaced by gastric mucus-producing cells. Pepsinogen I and II, gastrin, somatostatin, and $H^+/K^+$ ATPase showed substantially lowered expression in mice exhibiting gastric tumorigenesis compared with untreated mice or mice treated singularly ($p < 0.001$; f = 315.9; Supplementary Fig. 2a-g). Gastrin, somatostatin, and $H^+/K^+$ ATPase are required for normal gastric mucosal development and parietal cell activation[15,16]. In mice exhibiting carcinogenesis, these biomolecules were almost completely ablated. As a result, a combination of alcohol and *H. pylori* directly accelerates loss of differentiated epithelial cell types, leading to chronic atrophic gastritis and eventually to gastric tumorigenesis. The combinatorial treatment shifts gastric tissue to a tumor phenotype with increased numbers of inflammatory cells found in the tumor gastric mucosa. This observation suggests that *H. pylori* or alcohol alone is not enough to cause gastric tumorigenesis; a combination is required to trigger the formation of submucosal glands and invasion of tumor cells.

This effect is associated with increased tumor progression due to substantially reduced expression of several gastric tumor suppressor genes (TSGs), including *Tff1* (0.329 ± 0.087), *Tff2* (0.218 ± 0.041), *Gkn1* (0.246 ± 0.080) and *Gkn2* (0.372 ± 0.135) in the mouse group that developed tumors compared to other groups ($p < 0.001$; Supplementary Fig. 3a-d). Loss of these gastric-specific TSGs promotes tumorigenesis[17,18,19]. *Tff1* and *Tff2* genes are upstream regulators of *gastrokine (Gkn)* gene expression. Therefore, loss of *Tff1 or Tff2* expression could lead to tumor growth[20]. These genes were substantially downregulated in mice exhibiting gastric tumors, and the reduction was associated with the combined treatment of alcohol and *H. pylori* infection. Overall, inhibition of *Tff1*, *Tff2*, *Gkn1,* and *Gkn2* is known to be associated with tumorigenesis[20,21].

The extent of gastric tissue damage was evaluated as well. We found that mice treated simultaneously with alcohol and *H. pylori* exhibited tumor development. These mice displayed significantly higher activities of malondialdehyde (MDA; 364.479 ± 34.583 mg/mL), myeloperoxidases (MPO; 0.548 ± 0.060 U/L), catalase (28.369 ± 2.392 U/mL), carbonyl (102.558 ± 19.085 nmol/mg), and lipoperoxidase (LPO; 173.853 ± 27.849 µmol/L) compared to mice treated with either *H. pylori* or alcohol alone ($p < 0.001$; Supplementary Fig. 4a-e). A combination of alcohol and *H. pylori* infection increases peroxidation processes and leads to the production of superoxide radicals and aldehydes, such as MDA, MPO, and hydrogen peroxide, that can form adducts with DNA and proteins. Subsequently, we proposed that *H. pylori* infection and alcohol metabolites, including acetaldehydes, aldehydes, and peroxides, damage DNA, DNA repair enzymes, and immune cell protein cytokines, resulting in gastric tissue damage[22,23,24].

To further elucidate the effect of alcohol intake and *H. pylori* infection on the development of gastric cancer, we used gastric tumors from mice treated with both *H. pylori* and alcohol to develop a mouse xenograft model (MDX). We successfully developed the MDX model with tumors at the first (M1 = 100%) and second (M2 = 100%) passages (Supplementary Fig. 5a-d). Histological analysis further confirmed the tumorigenicity and gastric origin of this combination by showing high expression levels of cytokeratin (PCK-26; 0.860 ± 0.046, 0.714 ± 0.071, 0.792 ± 0.069) and low expression levels of vimentin (0.082 ± 0.005, 0.077 ± 0.004, 0.089 ± 0.004) and SMA-α (0.056 ± 0.018, 0.080 ± 0.023, 0.060 ± 0.021) in M0, M1, and M2 tumor tissues, respectively ($p < 0.001$; Supplementary Fig. 5e, f).

## 2.2. Alcohol dose in mice is relevant to human alcohol consumption and stage-dependent gastric cancer development

To apply our observations to humans, we optimized the mice's alcohol intake to reflect human intake to determine the dose-dependent (0.5-5 g/kg/day) effect of alcohol consumption. Mice treated with a combination of *H. pylori* infection and alcohol developed gastritis, leading to cancer in a dose-dependent manner (Fig. 2a, also 2g). A dose greater than 3.5 g/kg/day showed significant gastric carcinogenesis. Consequently, we treated mice with 5 g alcohol/kg/day to induce gastric carcinogenesis. This dose is non-toxic, and more importantly, it is comparable to the alcohol consumption of human gastric cancer patients (0.405 g/kg/day)[8]. These results suggest that alcohol dosage contributes substantially to the development of gastric inflammation and carcinogenesis.

We also examined alcohol intake, metabolism, and excretion and found a high blood assimilation of alcohol in mice with gastritis (0.344 ± 0.024 g/kg/day) or gastric tumors (0.654 ± 0.041 g/kg/day) compared to mice treated only with alcohol (0.074 ± 0.027 g/kg/day; $p < 0.001$). This observation corresponded with low urine dissimilation of alcohol in the gastric tumor group (0.103 ± 0.012 g/kg/day) compared to the gastritis group (0.181 ± 0.011 g/kg/day) or the group treated with only alcohol (0.620 ± 0.066 g/kg/day; $p < 0.001$). Similar results were found in human samples; gastric cancer patients (0.025 ± 0.000 g/kg/day) and chronic gastritis patients (0.022 ± 0.001g/kg/day) showed high levels of alcohol blood assimilation compared to healthy subjects (0.005 ± 0.001g/kg/day; $p < 0.001$; Fig. 2b, c). Alcohol dehydrogenase (i.e., an alcohol metabolizing enzyme) activity was significantly higher in mice exhibiting gastric tumorigenesis (93.259 ± 15.213 U/mL) compared to mice with the cohort treated with only alcohol (34.829 ±10.132 U/mL; $p < 0.001$; Fig. 2d). Moreover, mice with gastritis and gastric tumorigenesis exhibited a dark brown urine color with alkaline pH (Fig. 2e, f), suggesting the presence of a high level of alcohol dehydrogenase (ADH). These results also confirmed the role of alcohol consumption in the development of physiological abnormalities and gastric cancer.

High levels of ADH metabolites in urine following alcohol consumption may be a sign of gastric tumor development as well. The risk for alcohol-related cancer is influenced by the expression of alcohol metabolizing enzymes, such as ADH. Many Chinese, Korean, and Japanese individuals carry a version of the gene for ADH that codes for an overactive form of the enzyme[25]. This overactive ADH enzyme

speeds the conversion of alcohol (ethanol) to toxic acetaldehydes[26,27] and increases the risk for cancers like pancreatic, esophageal, liver, colorectal, and female breast cancers[28]. As a result, epidemiologists have regarded alcohol and acetaldehydes as potential carcinogens[10,29]. Ultimately, we developed a mouse model that utilizes an alcohol dosage relevant to human alcohol intake. With this model, gastric tumorigenesis is induced without toxicity in peripheral organs (Fig. 2g). As expected, activities of major alcohol metabolites (Acetaldehyde) were increased after combinational treatment of ethanol and *H .pylori* infection (45.382± 2.264 μM; $p < 0.0001$; Fig. 2h). As a result, this mouse model was used to study the effect of alcohol and its metabolites on the development of gastric cancer.

### 2.3 IL-10 knockout accelerates tumor growth in alcohol-treated and *pylori*-infected mice

Gastric inflammation leads to gastric tumor development. In our mice model, the number of pro-inflammatory cell types was significantly increased (i.e., leukocyte infiltration), as observed by the numbers of activated macrophages (F4/80 positive) and neutrophils (myeloperoxidases, MPO) in mice exhibiting gastric tumors (0.864 ± 0.037 and 0.912 ± 0.033, respectively), compared to untreated mice or mice treated with only alcohol or *H. pylori* (f = 86.65; $p < 0.001$; Supplementary Fig. 6a-c). Due to increased immunocyte infiltration, we analyzed several inflammatory-related chemokines and cytokines at the mRNA and protein (secretion) levels by qPCR and a customized multiplex magnetic bead array. In mice treated with alcohol and *H. pylori*, gastric tumorigenesis was associated with augmented Th1 (IFN-γ, IL-1β and GM-CSF) and Th2 (IL-10, IL-6, IL-13) cytokine expression ($p < 0.001$; Supplementary Fig. 7A-L). In particular, the anti-inflammatory cytokine interleukin-10 (IL-10) showed low expression in mice with gastric cancer. Similarly, IL-10 levels showed reduction in human gastric cancer and gastritis serum samples compared to healthy subjects ($p < 0.001$; Fig. 3a-g). Our data suggested that alcohol intake combined with *H. pylori* infection causes a marked imbalance in IL-10 cytokine levels ($p < 0.001$; Fig. 3a-g). We evaluated the association of gastric cancer with the combination of *H. pylori* and alcohol consumption. Figure 4H shows the ROC-curve for the discrimination IL-10 and *H. pylori* expression status with alcohol consumption data. The area under the curve (AUC) was found to be HP (area: 0.927, CI: 0.860-0.994), Cancer stage (area: 0.836, CI: 0.740-0.931) and IL-10 (area: 0.939, CI: 0.882-0.996) were associated with alcohol consumption (Supplementary Tables 1). Overall, the *H. pylori* infection and alcohol consumption showed great sensitivity and specificity towards IL-10; especially this combination could be used to confirmation of gastric cancer development.

We further examined the functional impact of IL-10 loss on gastric inflammation leading to gastric tumorigenesis induced by the combination of *H. pylori* infection and alcohol consumption. IL-10 ablation accelerated the development of gastric tumorigenesis in mice carrying IL-10-null alleles (Fig. 4a). Macroscopic morphometric analysis revealed that loss of the IL-10 gene accelerated the process of tumor development in mice treated with a combination of alcohol and *H. pylori* infection up to 32 weeks ($p < 0.0001$; Fig. 4b). These data support the view that IL-10 might act locally to resist chronic gastritis and subsequent gastric tumor development. We analyzed IL-$10^{-/-}$ mice for changes in acetaldehyde, $CD8^{+}$

cells and IL-1β levels, after alcohol or *H. pylori* stimulation. IL-$10^{-/-}$ mice treated with alcohol and *H. pylori* showed high acetaldehyde levels compared to mice treated alcohol or *H. pylori* alone or wild-type (WT) ($p < 0.0001$; Fig. 4c-e). Furthermore, the immune and inflammatory profile of IL-10 KO mice was analyzed by quantifying $CD8^+$ cells and IL-1β secretion in IL-10 knockout mice treated with alcohol and *H. pylori* infection. We found significantly diminished numbers of $CD8^+$ immune cells ($p < 0.0001$; Fig. 4f-h) and elevated IL-1β secretion ($p < 0.0001$; Fig. 5i-k) in mice treated combinatorically (Fig. 4l).

## 2.4 IL-10–deficient $CD8^+$ cells exhibit altered metabolic profiles after *pylori* infection and acetaldehyde stimulation

Functional mitochondria are crucial for tumor maintenance[30,31]. However, the role of mitochondria in immune cell function is largely unknown. Consequently, we examined the mitochondrial respiratory capacity of immune cells. We analyzed the effect of alcohol and *H. pylori* in several immune cell types: macrophages (CD-11b), CD-4+, CD-8+, NK (CD-49b) and B-cells (CD-19) and dendritic cells (CD-11c) (Supplementary Fig. 8a-f). For instance, IL-10-/- mice showed greatly diminished $CD8^+$ percentages compared to WT mice upon alcohol metabolite and/or *H. pylori* addition ($p < 0.0001$; Fig. 4f-h).

Furthermore, we analyzed the effect of alcohol consumption and *H. pylori* infection on mitochondrial protein by mRNA sequencing. RNA sequencing (RNA-seq) data showed that phosphoglycerate mutase (PGM2) predominantly expressed in WT group compared to mice treated with alone alcohol, *H. pylori*, or both alcohol and *H. pylori*) as well as 6-phosphofructo-2-kinase/fructose-2, 6-biphosphatase 3 (Pfkfb3). However, PGM2 expression was affected by IL-10 production ($p < 0.001$; Fig. 5A). PGM2 is a glycolytic enzyme, whereas *pfkfb3* gene has the highest kinase and phosphatase activity ratio, which in turn sustains high glycolytic rates. As a result, we investigated whether ablation of IL-10 signaling inhibits PGM2 expression in $IL10^{-/-}$ cells. To test this, we analyzed PGM2expression at the mRNA level in $IL\text{-}10^{-/-}$ mice. PGM2 expression was downregulated by IL-10 knockdown after alcohol stimulation and *H. pylori* infection ($p < 0.0002$; Fig. 5b-d). These data illustrate that IL-10 critically play an important role in regulate the glycolitic flux through glucose metabolism.

We subsequently investigated whether the altered mitochondrial metabolic profiles in IL-$10^{-/-}$ T-lymphocytes resulted from abnormal oxidative phosphorylation (OXPHOS). IL-$10^{-/-}$ T-lymphocytes ($CD8^+$) exhibited less oxidative phosphorylation compared with wild-type (WT) T-lymphocytes ($CD8^+$). However, the presence of exogenous IL-10 in IL-$10^{-/-}$ T-lymphocytes ($CD8^+$) after acetaldehyde (alcohol metabolite) or *H. pylori* stimulation resulted in increased oxidative phosphorylation ($p < 0.0001$; Fig. 5e-f). Furthermore, we measured Nitric oxide (NO) production in acetaldehyde and *H. pylori* stimulated T-lymphocytes. Higher NO production and addition of exogenous IL-10 restored the WT phenotype in IL-$10^{-/-}$ cells ($p < 0.001$; Supplementary Fig. 9a-d). Consequently, the reduction of oxidative phosphorylation in IL-$10^{-/-}$ cells is not due to nitric oxide production, since treatment with inhibitors of inducible nitric

oxide synthase failed to rescue the phenotype. Instead, addition of exogenous IL-10 restored the WT phenotype in IL-10−/− cells[30].

We next asked whether the inhibition of glycolysis by IL-10 is due to suppression of glycolytic flux. RNA-sequencing data showed that mice treated with both alcohol and *H. pylori* predominantly expressed Glut1 and Glut10 compared to mice treated with alcohol or *H. pylori* alone ($p < 0.0001$; Supplementary Fig. 10a-c). Specifically, Glut-10 expression was perturbed in IL-$10^{-/-}$ $CD8^+$ cells with stimulation of acetaldehyde and *H. pylori* infection. However, in the absence of exogenous IL-10, glucose uptake was maintained at higher levels in IL-$10^{-/-}$ $CD8^+$ cells. In contrast, in the presence of exogenous IL-10, glucose uptake was reduced in IL-$10^{-/-}$ $CD8^+$ cells ($p < 0.0001$; Supplementary Fig. 10d-e).

Additionally, PKM2 production was elevated in alcohol + *H. pylori* infected IL-$10^{-/-}$ mice (Fig. 5e). Lactate dehydrogenase levels were elevated as well (LDH-a & LDH-b), ($p < 0.0001$; Supplementary Fig. 11a-b). Higher glucose uptake was likely utilized for lactic acid fermentation by *H. pylori*, since only alcohol-treated mice showed low glucose uptake and low levels of lactate dehydrogenase production ($p < 0.0001$; Supplementary Fig. 10a-c). High glucose uptake shifts mitochondrial metabolism from oxidative phosphorylation to glycolysis in IL-$10^{-/-}$ CD8 cells, which accounts for the decrease in oxidative phosphorylation and CD8+ cell population discussed previously (Fig. 5e-f). Previous studies also demonstrate that IL-10 inhibits glucose translocation via downregulation of glycolytic gene expression[30]. Our RNA-seq analysis in IL-10 KO mice revealed that IL-10 inhibits gene expression of mitochondrial glycolytic pathway enzymes, including Aco, Pgm2, Mot2, Fabp, Mdh1, Glut, Pdk2 and Pfkp (Fig. 5a). Together, these data illustrate that IL-10 inhibits glycolytic flux by regulating GLUT10, a glucose transporter and gene expression of glycolytic enzymes.

IL-$10^{-/-}$ T-lymphocytes ($CD8^+$) were also analyzed for changes in mitochondrial content, total reactive oxygen species (ROS), and mitochondrial ROS production. IL-$10^{-/-}$ T-lymphocytes exhibited decreased mitochondrial mass after acetaldehyde (500 μM) plus *H. pylori* ($1x10^3$ cells/mL) stimulation compared to WT T-lymphocytes or cells treated with acetaldehyde or *H. pylori* stimulation alone ($p < 0.001$; Supplementary Fig. 12a-c). The reduction in mitochondrial content could be due to apoptosis and clearance of dysfunctional mitochondria (MitoTracker Green+high) with loss of $\Delta\psi m$ under acetaldehyde + *H. pylori* stimulation (Fig. 5i). Loss of $\Delta\psi m$ is associated with accumulation of mitochondrial reactive oxygen species. We therefore examined whether accumulation of $\Delta\psi m$ low mitochondria in IL-$10^{-/-}$ T-lymphocytes was associated with ROS production. Mitochondrial membrane potentials (MitoSox assay) were elevated in T-lymphocytes cells treated with acetaldehyde and *H. pylori* in the absence of IL-10 ($p < 0.01$; Supplementary Fig. 13a-c). We evaluated ROS levels through activation of the electron transport chain (ETC) in mitochondria. Hydrogen peroxide ($H_2O_2$) and mitochondrial superoxide levels were elevated in T-lymphocytes cells with combinatorial treatment compared to single treatment or WT ($p < 0.001$; Supplementary Fig. 14a-c). To assess ROS levels, we used the total ROS and mitochondria-specific ROS indicator DCFDA and MitoSox staining, respectively, to selectively detect mitochondrial superoxide. Total ROS and mitochondrial ROS production was enhanced in the absence of exogenous IL-10 and

inhibited in the presence of exogenous IL-10. This observation correlated with total mitochondrial mass. The accumulation of ROS-producing mitochondria in IL-10$^{-/-}$ cells was also visualized via live-cell imaging with fluorescent dyes, MitoTracker Green and MitoSox. Under alcohol and *H. pylori* stimulation, the absence of IL-10 resulted in lowered maximal respiratory capacity (MRC) compared with untreated CD8 cells. As a result, loss of mitochondrial fitness could be responsible for reduced IL-10 levels in CD8$^{+}$ cells after alcohol treatment and *H. pylori* infection. Consistent with this idea, basal cellular MitoSox levels were also reduced in CD8$^{+}$ cells after acetaldehyde and *H. pylori* infection. These data demonstrate metabolic reprogramming and altered ROS production as a consequence of combinational treatment of acetaldehyde (alcohol metabolite) and *H. pylori*. This combinatorial treatment contributes to metabolic dysfunction in CD8$^{+}$ cells, leading to lowered host immunity and increased inflammation. We also assessed the functional profile of mitochondria based on cytokine levels in IL-10$^{-/-}$ CD8$^{+}$ (Fig. 5g) and IL-10$^{-/-}$ CD11b$^{+}$ cells ($p < 0.001$; Supplementary Fig. 15a) by qPCR. IL-1β levels were elevated in combinatorial treatment of acetaldehyde and *H. pylori* compared to WT or IL-10$^{-/-}$ CD8$^{+}$ cells treated singularly($p < 0.0001$; Fig. 5h). IL-1β secretion was caspase-1–dependent. Exogenous IL-10 reverse the mito-dysfunction and switch from glycolysis to oxidative phosphorylation and leading to survival of CD8$^{+}$ cells with low gastric inflammation. As a result, we hypothesized that enhanced mitochondrial ROS production in IL-10$^{-/-}$ cells serves as an endogenous signal for inflammasome activation[30].

### 2.5 Ablation of IL-10 signaling lowers host immunity (CD8$^{+}$) and promotes *pylori* infection

We quantified the colony forming units of *H. pylori* in IL-10$^{-/-}$ mice treated with alcohol; there was no significance difference between treatment groups and WT ($p < 0.001$; Fig. 6a-c). These results suggest that IL-10 expression has no significant effect on *H. pylori* growth or cell number. We also examined the rate of *H. pylori* infection by measuring *H. pylori* secretions like CagA toxin ($p < 0.001$; Fig. 6d-f) and urease enzyme ($p < 0.001$; Supplementary Fig. 16a-c) in IL-10$^{-/-}$ cells stimulated with alcohol and *H. pylori* infection. Urease and CagA toxin secretion was enhanced in alcohol plus *H. pylori*-stimulated IL-10 knockout mice compared to those treated with *H. pylori* alone or WT.

We investigated the dose dependent effect of alcohol consumption on IL-10 and CD8$^{+}$ inhibition and *H. pylori* CagA infection. We found gradual decrease of CD8$^{+}$ and IL-10 levels in gastric cancer mouse model treated with continuing increase of alcohol dose (0.5-5g/kg/day) ($p < 0.001$; Fig. 6g-h). In contrast, *H. pylori* CagA infection was stimulated at high doses of alcohol ($p < 0.001$; Fig. 6i). These data suggest that alcohol consumption is strongly associated with the loss of IL-10 expression and lowered CD8$^{+}$ cell count, resulting in low host immunity. As a result, we investigated whether ablation of IL-10 signaling promotes *H. pylori* infection in low immune environments in gastric mucosae[32]. To test this, we analyzed the expression of CagA mRNA in IL-10$^{-/-}$ AGS gastric cancer cells stimulated with acetaldehyde, *H. pylori*, and IL-1β. CagA levels were dramatically increased in IL-10$^{-/-}$ cells compared to wild-type (WT) AGS gastric cancer cells ($p < 0.001$; Fig. 6j-k). Overall, these data illustrate that the tumor

microenvironment is influenced by acetaldehyde (alcohol metabolites) and *H. pylori* infection with IL-10 ablation and IL-1β overexpression, ultimately leading to reduced $CD8^+$ cell count (low immunity) and stimulation of *H. pylori* infection (Fig. 6l).

### 2.6 NKX6.3 downregulation results in gastric cancer cell survival and proliferation

NKX6.3 downregulation in IL-$10^{-/-}$ mice also plays a role in gastric carcinogenesis. We analyzed the effect of alcohol consumption and *H. pylori* infection on cancer protein by mRNA sequencing. RNA sequencing (RNA-seq) data showed that NKX6.3 predominantly expressed in WT group compared to mice treated with alone alcohol, *H. pylori*, or both alcohol and *H. pylori*). However, NKX6.3 expression was affected by IL-10 production ($p < 0.001$; Fig. 7a). However, *Lce3et* showed significantly higher mRNA expression in the combined treatment group as well ($p < 0.001$; Supplementary Fig. 17b-d). As a result, we investigated whether ablation of IL-10 signaling inhibits NKX6.3 expression in cells. To test this, we analyzed NKX6.3 expression at the mRNA level in IL-$10^{-/-}$ mice and at mRNA level. NKX6.3 expression was downregulated by IL-10 knockdown after alcohol stimulation and *H. pylori* infection ($p < 0.0001$; Fig. 7b-d). These data illustrate that IL-10 critically play an important role in gastric cancer cell proliferation by regulating NKX6.3 protein. NKX6.3 transfectants of $NCIN87^{NKX6.3}$ gastric cancer cells showed low NKX6.3 expression after addition of acetaldehyde, *H. pylori*, or IL-1β (Figure 7e). After treatment resulting in NKX6.3 downregulation, cell proliferation increased (Figure 7f), suggesting that NKX6.3 downregulation in IL-$10^{-/-}$ mice is involved in cancer cell proliferation.

NKX6.3-induced apoptosis in NCIN87NKX6.3 cells was stimulated with combination of acetaldehyde, *H. pylori*, or IL-1β (Figure 7g). Cleaved caspase 3 activity was enhanced with combination treatment of acetaldehyde, *H. pylori*, and IL-1β (Figure 7e). As shown in Figure 8, NKX6.3 expression had an effect on G1 and G2/M cell cycle progression (Figure 7h). Gastric cancer tissue samples displayed significantly higher NKX6.3 and IL-1β expression compared to samples from chronic gastritis and normal subjects ($p < 0.001$; Figure. 7i-j). These results suggest that acetaldehyde and *H. pylori* infection cause gastric tumorigenesis via NKX6.3 downregulation and IL-1β stimulation (Figure 7k).

# 3. Discussion

Gastric cancer begins with inflammation and progresses to gastritis and later to gastric carcinogenesis[33]. Our mouse model confirms the contribution of alcohol in the induction of gastric inflammation leading to gastric cancer in the presence of *H. pylori (*Fig: 1 & 2). In addition, the effects of interleukin–10 inhibition suggest that pre-existing gastric immunopathology accelerates the loss of differentiated epithelial cell types leading to profound glandular atrophy and gastric tumorigenesis. In

sum, IL–10 depletion may promote the shift from gastric inflammation to gastric carcinogenesis in mice treated with a combination of alcohol and *H. pylori* infection (Fig: 3 & 4).

Using mouse models, this study is the first to provide experimental evidence for the epidemiological link between high gastric cancer incidence and regions with high alcohol consumption and *H. pylori* infection[8]. This study also reveals the critical role of interleukin–10 in lowered host immunity via CD8+ cell downregulation and IL–1β upregulation. Defects in IL–10 regulation can result in mitochondrial dysfunction, observed as a metabolic shift from oxidative phosphorylation to glycolysis in activated T-lymphocytes (CD8+). In these pro-inflammatory conditions, gastric tumor suppressor gene (NKX6.3) expression is downregulated as well, resulting in increased gastric cancer cell survival and proliferation. As a result, stimulation of anti-inflammatory cytokine IL–10 can serve as a therapy against gastric cancer, in addition to lowered alcohol intake and pathogen clearance via antibiotic treatment. Gastritis patients with low IL–10 levels could also benefit from IL–10 stimulation as a possible preventive measure against gastric carcinogenesis (Fig: 5).

Beyond the clinical applications of this work, this study provides insight into the molecular mechanisms of gastric tumorigenesis. In mice, alcohol metabolites, such as peroxides or acetaldehydes, bind to immune cell GABAA receptors that in turn dysregulate and degrade immune cell populations (e.g., CD8 and CD4) and anti-inflammatory cytokines (e.g., IL–10) by metabolic reprogramming. Lowered host immunity promotes *H. pylori* infection of gastric cells, which further inflames gastric tissue (Fig. 5a). Here we provide evidence for IL–10–dependent regulation of glucose metabolism, mitochondrial metabolism and inflammatory responses in activated CD8+ cells. For example, upon alcohol activation, IL–10–deficient T-lymphocytes (CD8+) exhibited reduced oxidative phosphorylation (OXPHOS). The reduction in OXPHOS also coincided with elevated glucose uptake (e.g. GLUT10) for lactic acid fermentation under *H. pylori* infection with alcohol stimulation (e.g. LDHA). This metabolic shift leads to lactate production via PKM2 and LDH-A activation in IL–10-/- deficient T-lymphocytes[34,35,36]. Exogenous IL–10 blocks GLUT–10, PKM2 and LDH-A, decreasing glycolysis by lactate production and restoring oxidative phosphorylation activity. These data combined suggested that IL–10 uses an alternative metabolic pathway to sustain CD8+ cells mitochondrial activity, like glutamine As a result; ablation of IL–10 signaling perturbs glucose metabolism by dysregulating the PGM2, PFKFB3, and PKM2 expression and affects mitochondrial metabolism since glucose is not more an available metabolic substrate. Mitochondrial dysfunction also explains CD8+ cell death in IL–10–deficient mice (Fig. 5). As a result, *H. pylori* infection is exacerbated by low host immunity. Pathogen-induced inflammation is coupled with increased IL–1β secretion in IL–10-/- CD8+ cells with mitochondrial dysfunction. This chronic inflammation predisposes gastric cells towards carcinogenesis (Fig: 6).

Increased IL–1β expression promotes gastric inflammation and gastric cancer via regulation of NKX6.3 tumor suppressor gene. NKX6.3 is expressed in distal stomach epithelium[37]. Stable NKX6.3 expression induces apoptosis and enhances caspase–3 activity in NCIN87NKX6.3 cells; however, NKX6.3 gene expression is downregulated by acetaldehyde, *H. pylori* infection, and IL–1β production. As a result, of NKX6.3 downregulation, gastric cancer cell survival and proliferation is increased. We conclude that

NKX6.3 acts as a tumor suppressor gene involved in maintenance of gastric homeostasis and prevention of gastric tumorigenesis (Fig: 7).

# 4. Conclusions

In sum, many molecular mechanisms contribute to gastric carcinogenesis. Here we outline the synergistic effects of cytokine production (i.e. IL–10 and IL–1β), T-lymphocyte dysfunction, *H. pylori* infection and alcohol consumption on gastric cancer development and progression. In the future, these mechanisms and their molecular targets offer treatment opportunities for alcohol-associated gastric cancer.

# 5. Methods

## 5.1. Animal model experimental design

Mice were eight-week-old male C57-BL/6J-219 mice (18–20 g) (Beijing Vital River Laboratory, Beijing, China) and IL-$10^{+/-}$ and IL-$10F^{/+}$ mice (Stock code 004333, Jackson Laboratory, Bar Harbor, ME, USA). The experiments were performed after protocol approval by the ethics committee of China-US Hormel Cancer Institute, Henan, China and were conducted in accordance with the current guidelines for laboratory animal care. C57-BL/6J-219 (Access No: CUHCI2015006) and IL-10-mutant mice (Access No: CUHCI2015007) were randomly assigned to five groups of 10 animals each (n = 10). IL-$10^{-/-}$ and IL-$10F^{/+}$ heterozygous mice were crossed to obtain IL-$10^{+/+}$, IL-$10^{-/+}$ and IL-$10^{-/-}$ mutant mice. After one week of acclimation, mice were administered ethanol (5 g/kg/day) in drinking water for two weeks prior to infection with *H. pylori*, and alcohol administration was continued throughout the experiment. To facilitate *H. pylori* colonization, pantoprazole (20 mg/kg) was administered by gavage 3 times to lower gastric acidity. Each mouse was administered a suspension of *H. pylori* SS1 strain containing $10^8$ CFUs/mL by gavage 3 times per week. Mice (n = 5) were euthanized on consecutive weeks of 4, 8, 12, 16, 20, 24, 28, 32, 36, and 40 weeks. A control group was maintained without any treatment. Doses of alcohol ranging from 0.5–5.0 g/kg/day were administered to mice (n = 5) to determine the optimal alcohol dose to induce gastric tumorigenesis.

## 5.2. Patients and gastroendoscopy

All gastric patients were subjected to gastroendoscopy and examination in the Second Affiliated Zhengzhou University Hospital and Henan Cancer Hospital (Zhengzhou, Henan, China). Blood samples and tissue biopsies were obtained from consenting patients from the antral and corpus portions of the stomach during gastrointestinal endoscopy and gastric surgery. The patients who donated the primary tumors were completely informed and provided written consent (Access No: CUHCI2015009).

### 5.3. Immunohistochemistry (IHC)

Paraffin-embedded gastric tissues were analyzed by immunohistochemistry (IHC). Serial sections (4–6 mm each) were deparaffinized in xylene and rehydrated in an alcohol concentration gradient and evaluated with antibodies to detect *H. pylori* (1:100), pepsinogen I and II (1:100 each), MPO (1:100), F4/80 (1:100), vimentin (1:100), PCK-26 (1:100), NKX6.3 (1:100), IL-10 (1:100) and SMA-α (1:100). Sections were subsequently incubated with their respective secondary antibodies for 30 minutes at room temperature. The signal was visualized with peroxidase-labeled streptavidin complexes by DAB, and the sections were briefly counterstained with hematoxylin. The immunohistochemical localization pattern was also recorded by digital imaging (Nikon Ti-DS, Japan). ImageScope (11.1.1.752) software program was used, and the labeling index was calculated as a percentage of positive cells relative to the total number of counted cells.

### 5.4. Quantitative enzyme and activity assays

Quantitative enzyme assays included measurement of Nitrite (Cayman, Michigan, USA, Cat number 780001), Aldehyde (Abcam, Cambridge, MA, USA, Cat number ab138882), urease (Cat number C013-2), malondialdehyde (MDA; Cat number A003-1), myeloperoxidase (MPO; Cat number A044), carbonyl (Cat number A087), lipoperoxidase (LPO), catalase (Cat number A007-1) and alcohol dehydrogenase (ADH; Cat number A083-1) were performed according to the manufacturer's instructions (Nanjing Jiancheng Bioengineering Institute, Nanjing, China).

### 5.5. Enzyme-linked immunosorbent assay

Serological assessment of CD-8 (Abcam, Cambridge, MA, USA, Cat number ab 238264), *H. pylori* (BioCheck, San Francisco, CA, USA, Cat number BC-1051), and *H. pylori* CagA (MyBiosource, San Diego, CA, USA, Cat number MBS263962) were measured by enzyme-linked immunosorbent assay (ELISA). Commercial ELISA kits were used to analyze serological values of CD8, *H. pylori* and *H. pylori* CagA according to manufacturer's instructions (Cusabio, US).

### 5.6. Real-time RT-PCR

Total RNA was extracted using the commercial RNA extraction kit (Ambion by Life Technologies, Van Allen Way Carsbad, USA, 92008) and cDNA synthesized by amfiRivert cDNA synthesis platinum master mix (GenDEPOT, Katy, TX, USA, Cat number R5600-200). Real-time PCR (qRT-PCR) was conducted using a 7500 FastDX (Applied Biosystems, MA, USA) and the power SYBR green PCR master mix (Applied

biosystem, Warrington WA1 4SR, UK, Cat number 4367659). Primer IDs and sequences are shown in Supplementary Tables 2, 3 and 4.

### 5.7. Cytokine and chemokine protein measurement using a multiplex bead array.

Cytokine and chemokine protein levels in mouse (Cat number 740446) and human (Cat number 740118) serum were measured using a multiplex magnetic bead array kit (customized by BioLegend LEGENDplex, San Diego**,** CA, USA). The multiplex bead arrays were performed according to the manufacturer's instructions with a minimum detectable concentration varying from 0.96–11.27 pg/mL. Legendplex (version: 7.0) software program was used to analyze the FACS data and the cytokine concentrations were calculated in pg/mL against standard values.

### 5.8. *H. pylori* CFU quantification within Mouse Stomachs and Histology

After 1, 3, or 6 weeks, mice were euthanized. Stomachs were halved longitudinally along the greater and lesser curvatures and rinsed in sterile phosphate-buffered saline. Each half was manually disrupted on ice in 750 µL of Iso-Sensitest (Oxoid, Basingstoke, UK) broth/15% glycerol. Cells were serially diluted and plated on Columbia blood agar base plates (Oxoid, Basingstoke, UK, Cat number CM0331), supplemented with 10% defibrinated horse blood (Solarbio, Beijing, CRP, Cat number S9050), and Dent supplement (Oxoid, Basingstoke, UK, Cat number SR0147E).

### 5.9. Urine collection and measurement (metabolic cage experiments)

Alcohol metabolism and urinary flow rate were determined by placing mice individually in metabolic cages. Mice were allowed a 3-day habituation period to adapt to the environment. Later, food and water intake, urinary flow rate, and body weight were recorded every day. Subsequently, a 12 h collection (9 p.m. to 9 a.m.) of urine was performed to obtain the urinary parameters, including volume, pH, and color. Data were analyzed for alcohol intake, metabolism, and excretion. Alcohol content in the serum and urine samples from mice and humans was measured according to the Enzychrom ethanol commercial assay kit's instructions (BioAssay System, ECET-048, Hayward, CA, USA, Cat number ECET-048).

### 5.10. Mouse-derived xenograft model

A mouse-derived xenograft model was developed from gastric tumor tissue of mice treated with alcohol (Access No: CUHCI2016011). Then additional mice were subcutaneously implanted with tissues weighing

0.10-0.12 g and measuring ~3 mm. Animals were monitored periodically for their weight and tumor growth. A second passage was performed and the same protocol was followed as described above.

### 5.11. RNA-seq analysis

Total RNA of stomach tissues was prepared by using an RNeasy kit (QIAGEN) with an RNase free DNase set (QIAGEN). Sample preparation and sequencing were performed in the BGI (Beijing Genomics Institute, Shenzhen Beishan Industrial Zone, Shenzhen 518083, China) using an Illimina HiSeq sequencing system at 50 bp read length.

### 5.12. Cell culture

Jurkat T-lymphocytes, RAW264.7, NCIN87, AGS and HEK-293T cell lines were purchased from the American Type Culture Collection (Manassas, VA, USA) and cultured in DMEM, RPMI-1640 media supplemented with 10% FBS (Invitrogen, Camarillo, CA, US), 100 U/mL penicillin, and 100 µg/mL streptomycin. All the cell lines were authentified for mycoplasma; with the passage number of 3-5. The cell cultures were maintained at 37 ºC under 5% $CO_2$. Cells were seeded in 100 x 20 mm dish of DMEM/F12. Upon 70% confluence, cells were treated with acetaldehyde (500 µM), IL-1β and IL-10 (100ng/mL; Peprotech, Rocky Hill, USA, Cat number 200-01B), or infected with *H. pylori* strain (ATCC-43504) ($1x10^3$ bacteria/mL).

### 5.13. DNA constructs, transfection, and electroporation

A lentiviral expression system was used to knockdown IL-10 target protein in RAW 264.7 cells. HEK-293T cells were cultured in DMEM containing penicillin (100 units/mL), streptomycin (100 µg/mL), and 10% fetal bovine serum (FBS, Gemini Bio-Products, Calabasas, CA). Cell cultures were maintained at 37 °C under 5% $CO_2$ in a humidified atmosphere. Cytogenetically tested and authenticated frozen cells were thawed and maintained for approximately two months. HEK 293T cells were cultured in DMEM with 10% FBS.

For knockdown of IL-10 expression in RAW264.7 cells or HEK 293T cells, transfection was performed with *shRNA IL-10*, or *pLKO.1-mock* DNA plasmids together with packaging vectors, *pMD2.0G* and *psPAX* (Addgene Inc., Cambridge, MA). Imfectin Ploy DNA transfection reagent (GenDepot, Barker, Tx, USA, Cat number 17200-101,) was used as directed by the manufacturer's protocols. Transfection medium was changed at 4 h post-transfection, and the cells were cultured for an additional 36 h in fresh medium. Viral particles were harvested by filtration using a 0.45 mm syringe filter. Viral infection into RAW264.7 cells occurred with polybrene (1 µg/mL; Sigma-Aldrich, St. Louis, MO, USA, Cat number TR-1003-G) for 24 h.

Cell culture medium was replaced with fresh media, and the cells were cultured for an additional 24 h after selection with Puromycin (2 µg/mL; Gemini Bio Product, Cat number = 400128P). Furthermore, Bio-Rad electroporation system was used for knocking down the expression of IL-10 in Jurkat immune cells. Electroporation pulser cuvette (BioRad Gene Pulser, Cat number XCell, 617BR105102) was used with a protocol of voltage (V) = 10, Capacitance (µF) = 25, Resistance (Ω) = infinite, cuvette = 2mm (BioRad Gene Pulser Cuvette, Cat number 165-2086). Furthermore, NCIN87 gastric cancer cells lines were cultured at 37 °C under 5% $CO_2$ in RPMI-1640 medium with 10% heat-inactivated fetal bovine serum. Complete *NKX6.3*-cDNA (gene symbol= NKX6.3, Harvard Medical School, Clone ID = HsCD00461824) was cloned into the expression vector pCMV6-Myc-DDK (Origene). NCIN87 cells were transiently transfected with expression plasmids (15 µg total DNA) in 150 x 25 mm dishes using lmfectin Ploy DNA transfection reagent (GenDepot, Barker, Tx, USA, Cat number 17200-101), according to the manufacturer's recommendations. Stable expression of NKX6.3 was confirmed in NCIN87$^{NKX6.3}$ cells by Western Blot analysis. ShRNA and overexpression plasmid sequences are shown in Supplementary Tables 3.

### 5.14. Immunoblotting

Cells were washed with PBS (pH 7.4) and incubated with lysis buffer. Afterwards, samples were evaluated for anti-NKX6.3 (1:250), anti-Apoptosis Western-blot Cocktail (1:1000), anti-OXPHOS (1:1000);, anti-Pgm2 (1:250), anti-pkm2 (1:1000) and anti-GAPDH (1:250) as described [38, 39].

### 5.15. Tissue harvesting for cell sorting and FACS analysis

Mice stomach tissue was minced into 3-4 pieces and pressed firmly to force the fragments apart; this allowed cells to pass through a wire mesh (70 µM Nylon; Corning, Durham, USA, Cat number 431751,). The cell suspension was centrifuged at 250 x g for five minutes at room temperature. Each cell pellet was treated with ammonium chloride (0.17 M per 1 mL cell pellet) and incubated at room temperature for five minutes, followed by centrifugation at 250 x g for five minutes. The pellet was washed with PBS, and the cells were gently resuspended into Corning DMEM media. After washing with PBS containing 2% BSA, cells were incubated with a lineage cocktail containing biotinylated antibodies against CD4 (Biolegend, London, UK, Cat number 557307), CD8 (Biolegend; Cat number 553030), CD19 (Biolegend; Cat number 557398), CD11b (Biolegend; Cat number 561688), CD11c (Biolegend; Cat number 557400) and CD49b (Biolegend; Cat number 561067) at 4 °C for 30 minutes in the dark. After washing twice with PBS containing 1% FBS and 0.1% sodium azide, cell sorting was performed using a BD FACSAria II, San Jose, CA, SN: P69500099 cell sorter with BD FACSDiva Software version 8.0.2. Data were analyzed with BD FlowJo version 10 software.

### 5.16. Measurement of mitochondrial activity and ROS production

Jurkat T-lymphocytes cells seeded in non-tissue culture plates were stimulated as described above. MitoTracker Green (0.3uM; Molecular probes, Isnvitrogen Oregon USA, Leiden Netherland, Cat number CM-H2Xros) (for total mitochondrial mass), Total ROS (DCFDA) (0.1uM; Sigma Aldrich, St. Louis, MO, USA, Cat number D6883-250MG), and MitoSox staining (5uM; MitoSox Red mitochondrial superoxide indicator, Invitrogen by Thermo-Fisher Scientific, Cat number M36008), were performed according to manufacturer's instructions. For flow cytometry analysis, data were acquired with a BD FACSAria II, San Jose, CA, SN: P69500099 cell sorter with BD FACSDiva Software version 8.0.2. Data were analyzed with BD FlowJo version 10 software.

### 5.17. Cell proliferation and viability assay

Cells ($1 \times 10^3$ cells/well) were plated in 96-well plates. After 24 hours, cells were treated with the acetaldehyde (500 μM), *H. pylori* ($1 \times 10^3$ cells), or IL-1β (100 ng/mL) and incubated at 37 ºC for 24, 48, 72, or 96 hours. IncuCyteS3 live-cell imaging system (Essen BioScience, Tokyo, Japan, IC5047) was used to monitor cell proliferation. Later, IncuCyteS3:2019 software was used to quantify cell proliferation. This cell proliferation assay was performed in six replicates.

### 5.18. Apoptosis and cell cycle analysis via flow cytometry

For apoptosis assessment, an Annexin V-FITC (BD Pharmingen (BD Biosciences), Franklin Lake, NJ, USA, Cat number 556419) binding assay was performed in NCIN87$^{NKX6.3}$ cells stimulated with acetaldehyde (500uM; Sigma Aldrich, St. Louis, MO, USA, Cat number 402788-100ML), IL-1β (100ng/mL; Peprotech, Rocky Hill, USA, Cat number 200-01B) and *H. pylori* ($1x10^3$). For cell cycle analysis, the cells from each experimental group were harvested, fixed overnight in 70% ethanol, and stained with propidium iodide (50 ug/mL; BD Pharmingen (BD Biosciences), Franklin Lake, NJ, USA, Cat number 556463) and RNase (Sigma-Aldrich, St. Louis, MO, USA, Cat number R5125-250MG) for 30 minutes before analysis on a BD LSRFortessa X-20, San Jose, CA, SN: R656385195 with BD FACSDiva Software version 8.0.2. Data were analyzed with BD FlowJo version 10 software.

### 5.19. Statistical analysis

The experiments were randomized, and investigators were blinded to histological examination during all experiments. All statistical analyses were performed using Graphpad Prism 5.0 software (San Diego, CA, USA), with differences between groups considered significant with a *p value* <0.001. Data are presented as mean values ± S.E.M. Histopathological scores and all other experimental data were compared using

a t-test (two-sided) or one-way analysis of variance (ANOVA) followed by (post hoc) Newman-Keuls multiple and Turkey multiple comparison tests. The discriminatory ability of markers for gastric cancer was evaluated by Receiver Operating Characteristics Curve (ROC) providing the Area Under the Curve (AUC). All tests were two-sided and P-values≤ 0.01 were considered statistically significant. Statistical software IBM SPSS 20.0 (SPSS Inc., Chicago, IL) and R program package (Wirtschafts Universität, Wien, Austria) were used to perform these analyses.

# Abbreviations

ADH, alcohol dehydrogenase; *Gkns, Gastrokines;* HNE, hydroxynonenal; *H. pylori, Helicobacter pylori;* IARC, International Agency of Research on Cancer; IFN, interferon; IL, interleukin; LPO, lipoperoxidase; MDA, malondialdehyde; MDX, mouse xenograft model; MPO, myeloperoxidases; SMA-α, smooth muscle antigen; *Tff1, Trefoil factor1; Tff2, Trefoil factor2;* TNF, tumor necrosis factor; TSGs, tumor suppressor genes; WHO, World Health Organization.

# Declarations

### Ethics approval and consent to participate

The institutional review board at China-US Hormel Cancer institute approved the study. Subjects provided informed consent to be included

### Consent for publication

All experiments were approved by the ethics committee of The Affiliated Cancer Hospital Affiliated to Zhengzhou University, Henan, P. R. China. Written informed consent was got from every patient before the start of our research.

### Data availability

All data needed to evaluate the conclusions of this paper are present in the paper and/or Supplementary Materials. The source data underlying Figs 2a–d, 3a–c, 4a, c, 5b–f, and 6b and Supplementary Figs S1a–d, S2a–g, S3a–d, S4a–e, S5a–f, S6a–c, S7a–l, b, S8a–f, S9a–d, S10a–e, S11a–b, S12a–c, S13a–c, S14a–c, S15, S16a–c and S17a–e are provided as Source Data files. All other data are available from the corresponding author (Z.D.) by request.

### Competing interests

None of the authors declare any competing interests.


## Funding

The project was supported by the National Natural Science Foundation of China (NSFC), Research Grant Nos. 81750110551 and 81572812.


## Author Contributions

F.A. designed and performed the experiments, derived the models and analyzed the data; F.A. and Z.D. conceived the idea. Z.D. supervised the project. F.A., A.C., H. Y. and J. M. analyzed the data and interpretate the results. K.L., G.X. and L.Y. provided the gastritis and gastric cancer patient's samples and characterized their pathology. F. A., R.B. and X. L. performed the pathological analysis of mouse tissue samples. F.A, wrote and A.M.B. edited the manuscript.


## Acknowledgments

Not applicable



## Author Information

Faisal Aziz: faziz@umn.edu

Abhijit Chakraborty: achakrab@umn.edu

Kangdong Liu: kdliu@hci-cn.org

Hisae Yoshitomi: hyoshito@umn.edu

Xiang Li: xli@hci-cn.org

Josh Monts: jmonts@umn.edu

Gang Xu: zyytyy1069@163.com

Yonghan Li: liyonghan1020@126.com

Ruihua Bai: brhlily@outlook.com

Ann M. Bode: ambode@hi.umn.edu or bodex008@umn.edu

Zigang Dong: dongx004@umn.edu or zgdong@hci-cn.org

# References

1 Aziz F, Sherwani SK, Akhtar SS, Kazmi SU. Development of an in-house enzyme-linked immunosorbent assay based on surface whole cell antigen for diagnosis of Helicobacter pylori infection in patients with gastroduodenal ulcer disease. *World J Microbiol Biotechnol.* 2014;30:305–15. https://doi.org/10.1007/s11274-013-1448-4.

2 Aziz F, Chen X, Yang X, Yan Q. Prevalence and Correlation with Clinical Diseases of Helicobacter pylori cagA and vacA Genotype among Gastric Patients from Northeast China . *Biomed Res Int* 2014;2014:1–7. https://doi.org/10.1155/2014/142980.

3 Aziz F, Yang X, Wen Q, Yan Q. A method for establishing human primary gastric epithelial cell culture from fresh surgical gastric tissues. *Mol Med Rep* 2015;12:2939–44. https://doi.org/10.3892/mmr.2015.3692.

4 Helicobacter pylori _ physiology and genetics (eBook, 2001) [WorldCat n.d.

5 Helicobacter pylori - Chapter 4 - 2020 Yellow Book _ Travelers' Health _ CDC n.d.

6 Group CC. Gastric cancer and Helicobacter pylori : a combined analysis of 12 case control studies nested within prospective cohorts 2001:347–53.

7 Bray F, Ferlay J, Soerjomataram I, Siegel RL, Torre LA, Jemal A. Global cancer statistics 2018: GLOBOCAN estimates of incidence and mortality worldwide for 36 cancers in 185 countries. *CA Cancer J Clin* 2018;68:394–424. https://doi.org/10.3322/caac.21492.

8 Moy KA, Fan Y, Wang R, Gao Y-T, Yu MC, Yuan J-M. Alcohol and tobacco use in relation to gastric cancer: a prospective study of men in Shanghai, China. *Cancer Epidemiol Biomarkers Prev* 2010;19:2287–97. https://doi.org/10.1158/1055-9965.EPI-10-0362.

9 Correa P, Houghton JM. Carcinogenesis of Helicobacter pylori. *Gastroenterology* 2007;133:659–72. https://doi.org/10.1053/j.gastro.2007.06.026.

10 IARC Working Group on the Evaluation of Carcinogenic Risks to Humans. Alcohol consumption and ethyl carbamate. *IARC Monogr Eval Carcinog Risks to Humans* 2010;96:542–602. https://doi.org/http://www.ncbi.nlm.nih.gov/pubmed/21735939.

11 Blot WJ, McLaughlin JK,Winn DM et al. Smoking and drinking in relation to oral and pharyngeal cancer. *Cancer Res* 1988;48:3282–7.

12 Couper KN, Blount DG, Riley EM. IL-10: The Master Regulator of Immunity to Infection 2019. https://doi.org/10.4049/jimmunol.180.9.5771.

13 IL-10_ The Master Regulator of Immunity to Infection _ The Journal of Immunology n.d.

14 Ouyang W, Garra AO. 25 Review IL-10 Family Cytokines IL-10 and IL-22 : from Basic Science to Clinical Translation. *Immunity* 2019;50:871–91. https://doi.org/10.1016/j.immuni.2019.03.020.

15 Khan ZE, Wang TC, Cui G, Chi AL, Dimaline R. Transcriptional regulation of the human trefoil factor, TFF1, by gastrin. *Gastroenterology* 2003;125:510–21. https://doi.org/10.1016/S0016-5085(03)00908-9.

16 Zavros Y, Eaton KA, Kang W, Rathinavelu S, Katukuri V, Kao JY, *et al.* Chronic gastritis in the hypochlorhydric gastrin-deficient mouse progresses to adenocarcinoma. *Oncogene* 2005;24:2354–66. https://doi.org/10.1038/sj.onc.1208407.

17 Martin G, Wex T, Treiber G, Malfertheiner P, Nardone G. Low-dose aspirin reduces the gene expression of gastrokine-1 in the antral mucosa of healthy subjects. *Aliment Pharmacol Ther* 2008;28:782–8. https://doi.org/10.1111/j.1365-2036.2008.03793.x.

18 Moss SF, Lee JW, Sabo E, Rubin AK, Rommel J, Westley BR, *et al.* Decreased expression of gastrokine 1 and the trefoil factor interacting protein TFIZ1/GKIM2 in gastric cancer: Influence of tumor histology and relationship to prognosis. *Clin Cancer Res* 2008;14:4161–7. https://doi.org/10.1158/1078-0432.CCR-07-4381.

19 Resnick MB, Sabo E, Meitner PA, Kim SS, Cho Y, Kim HK, *et al.* Global analysis of the human gastric epithelial transcriptome altered by Helicobacter pylori eradication in vivo. *Gut* 2006;55:1717–24. https://doi.org/10.1136/gut.2006.095646.

20 Westley BR, Griffin SM, May FEB. Interaction between TFF1, a gastric tumor suppressor trefoil protein, and TFIZ1, a brichos domain-containing protein with homology to SP-C. *Biochemistry* 2005;44:7967–75. https://doi.org/10.1021/bi047287n.

21 Peterson AJ, Menheniott TR, O'Connor L, Walduck AK, Fox JG, Kawakami K, *et al.* Helicobacter pylori infection promotes methylation and silencing of trefoil factor 2, leading to gastric tumor development in mice and humans. *Gastroenterology* 2010;139:2005–17. https://doi.org/10.1053/j.gastro.2010.08.043.

22 Baik S-C, Youn H-S, Chung M-H, Lee W-K, Cho M-J, Ko G-H, *et al.* Increased Oxidative DNA Damage in Helicobacter pylori-infected Human Gastric Mucosa. *Cancer Res* 1996;56:.

23 Federico A, Morgillo F, Tuccillo C, Ciardiello F, Loguercio C. Chronic inflammation and oxidative stress in human carcinogenesis. *Int J Cancer* 2007;121:2381–6. https://doi.org/10.1002/ijc.23192.

24 Tardieu D, Jaeg JP, Deloly a, Corpet DE, Cadet J, Petit CR. The COX-2 inhibitor nimesulide suppresses superoxide and 8-hydroxy-deoxyguanosine formation, and stimulates apoptosis in mucosa during early colonic inflammation in rats. *Carcinogenesis* 2000;21:973–6. https://doi.org/10.1093/carcin/21.5.973.

25 Druesne-Pecollo N, Tehard B, Mallet Y, Gerber M, Norat T, Hercberg S, *et al.* Alcohol and genetic polymorphisms: effect on risk of alcohol-related cancer. *Lancet Oncol* 2009;10:173–80. https://doi.org/10.1016/S1470-2045(09)70019-1.

26 Homann N, Jousimies-Somer H, Jokelainen K, Heine R, Salaspuro M. High acetaldehyde levels in saliva after ethanol consumption: Methodological aspects and pathogenetic implications. *Carcinogenesis* 1997;18:1739–43. https://doi.org/10.1093/carcin/18.9.1739.

27 Seitz HK, Simanowski UA, Garzon FT, Rideout JM, Peters TJ, Koch A, *et al.* Possible role of acetaldehyde in ethanol-related rectal cocarcinogenesis in the rat. *Gastroenterology* 1990;98:406–13. https://doi.org/10.1016/0016-5085(90)90832-L.

28 Kanda J, Matsuo K, Suzuki T, Kawase T, Hiraki A, Watanabe M, *et al.* Impact of alcohol consumption with polymorphisms in alcohol-metabolizing enzymes on pancreatic cancer risk in Japanese. *Cancer Sci* 2009;100:296–302. https://doi.org/10.1111/j.1349-7006.2008.01044.x.

29 Straif K, Lauby-secretan B, Baan R, Straif K, Grosse Y, Secretan B, *et al.* Carcinogenicity of alcoholic beverages Carcinogenicity of alcoholic beverages 2007;2045:7–9. https://doi.org/10.1016/S1470-2045(07)70099-2.

30 Ip WKE, Hoshi N, Shouval DS, Snapper S, Medzhitov R. Anti-inflammatory effect of IL-10 mediated by metabolic reprogramming of macrophages. *Science (80- )* 2017;356:513–9. https://doi.org/10.1126/science.aal3535.

31 Murray PJ. The primary mechanism of the IL-10-regulated antiinflammatory response is to selectively inhibit transcription. *Proc Natl Acad Sci* 2005;102:8686–91. https://doi.org/10.1073/pnas.0500419102.

32 Jiang P, Du W, Wu M. Regulation of the pentose phosphate pathway in cancer 2014;5:592–602. https://doi.org/10.1007/s13238-014-0082-8.

33 Correa P. Human Gastric Carcinogenesis: A Multistep and Multifactorial Process First American Cancer Society Award Lecture on Cancer Epidemiology and Prevention 1. *Cancer Res* 1992;52:6735–40. https://doi.org/10.1056/NEJMra020542.

34 Fischer K, Hoffmann P, Voelkl S, Meidenbauer N, Ammer J, Edinger M, *et al.* Inhibitory effect of tumor cell – derived lactic acid on human T cells 2019;109:3812–20. https://doi.org/10.1182/blood-2006-07-035972.The.

35 Buck MD, Sowell RT, Kaech SM, Pearce EL, Sciences B, Program I, *et al.* Metabolic Instruction of Immunity 2018;169:570–86. https://doi.org/10.1016/j.cell.2017.04.004.Metabolic.

36 Kroemer G, Pouyssegur J. Review Tumor Cell Metabolism : Cancer ' s Achilles ' Heel 2008. https://doi.org/10.1016/j.ccr.2008.05.005.

37 Yoon JH, Choi WS, Kim O, Choi SS, Lee EK, Nam SW, *et al.* NKX6 . 3 controls gastric differentiation and tumorigenesis 2015;6:.

38 Aziz F, Yang X, Wang X, Yan Q. Anti-LeY antibody enhances therapeutic efficacy of celecoxib against gastric cancer by downregulation of MAPKs/COX-2 signaling pathway: correlation with clinical study. *J Cancer Res Clin Oncol* 2015;141:. https://doi.org/10.1007/s00432-014-1892-z.

39 Aziz F, Wang X, Liu J, Yan Q. Ginsenoside Rg3 induces FUT4-mediated apoptosis in H. pylori CagA-treated gastric cancer cells by regulating SP1 and HSF1 expressions. *Toxicol Vitr* 2016;31:. https://doi.org/10.1016/j.tiv.2015.09.025.

# Figures

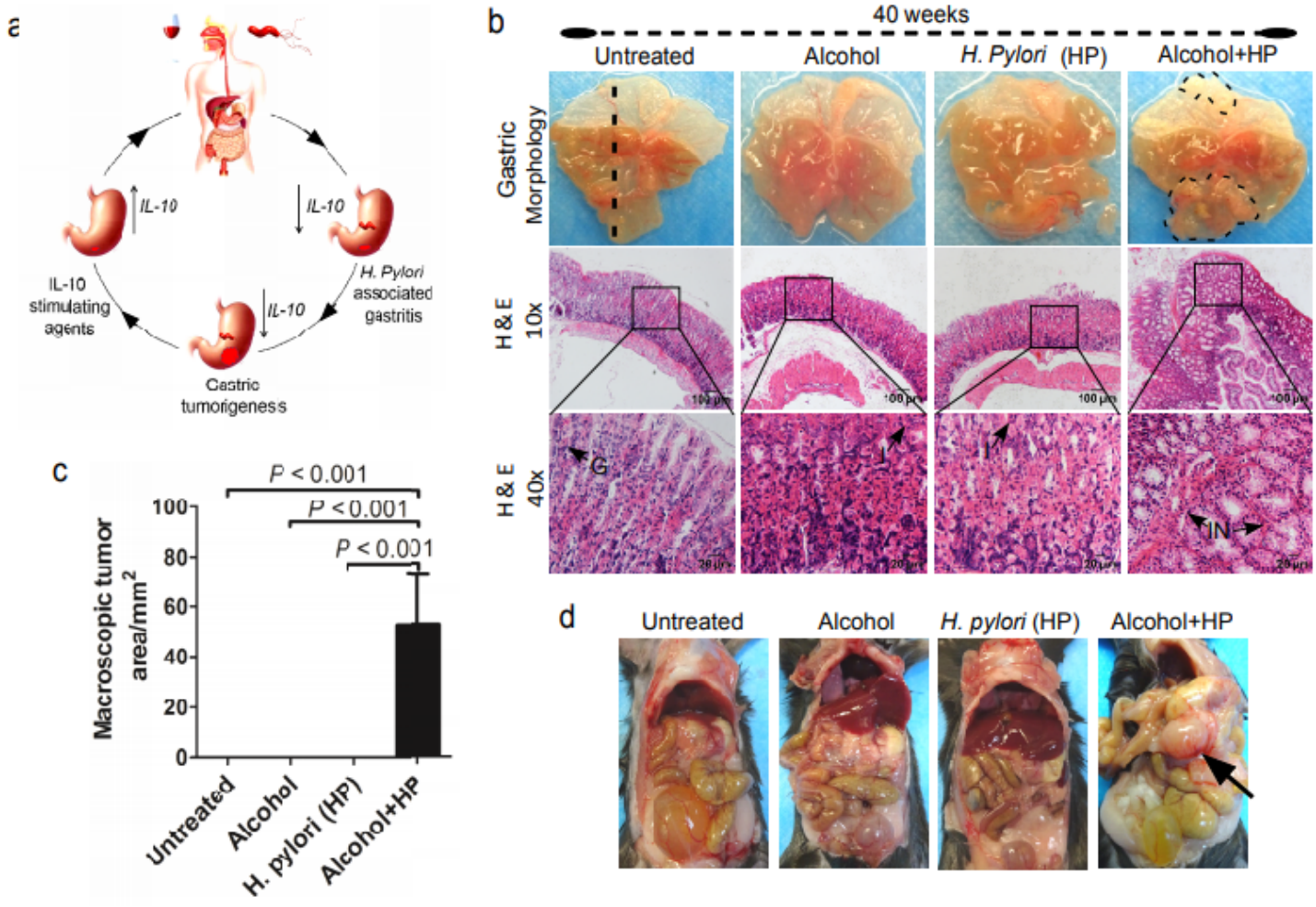

## Figure 1

Development of mice models for alcohol- and H. pylori-induced progression of gastritis to gastric cancer. a) Schematic drawing showing the effect of alcohol consumption and H. pylori infection in the development and progression of gastritis to gastric tumorigenesis mediated through the inhibition of IL-10. b) Macroscopic (top) and histologic (bottom) analyses of gastric mucosae (n = 5/cohort). Images of tumors at 40 weeks from mice infected with H. pylori and treated with alcohol; tumor areas are outlined with dotted circles. Hematoxylin and eosin (H&E) stained cross sections and cut along the fundus to the proximal end of the corpus as shown by the straight dotted line. Gastric pathology was substantially changed after 32 and 40 weeks of combination treatment with H. pylori and alcohol. The panels are magnified 10x (Bar, 100 μm) and 40x (Bar, 20 μm). Arrow and G= glandular zone, I= inflammatory cells, IN= muscular mucosae invasion. c) The size of gastric tumors from mice treated with alcohol and infected with H. pylori compared to mice treated with only alcohol or H. pylori is shown. d) Photographs of solid tumors (arrows) at 40 weeks from mice treated with alcohol and infected with H. pylori.

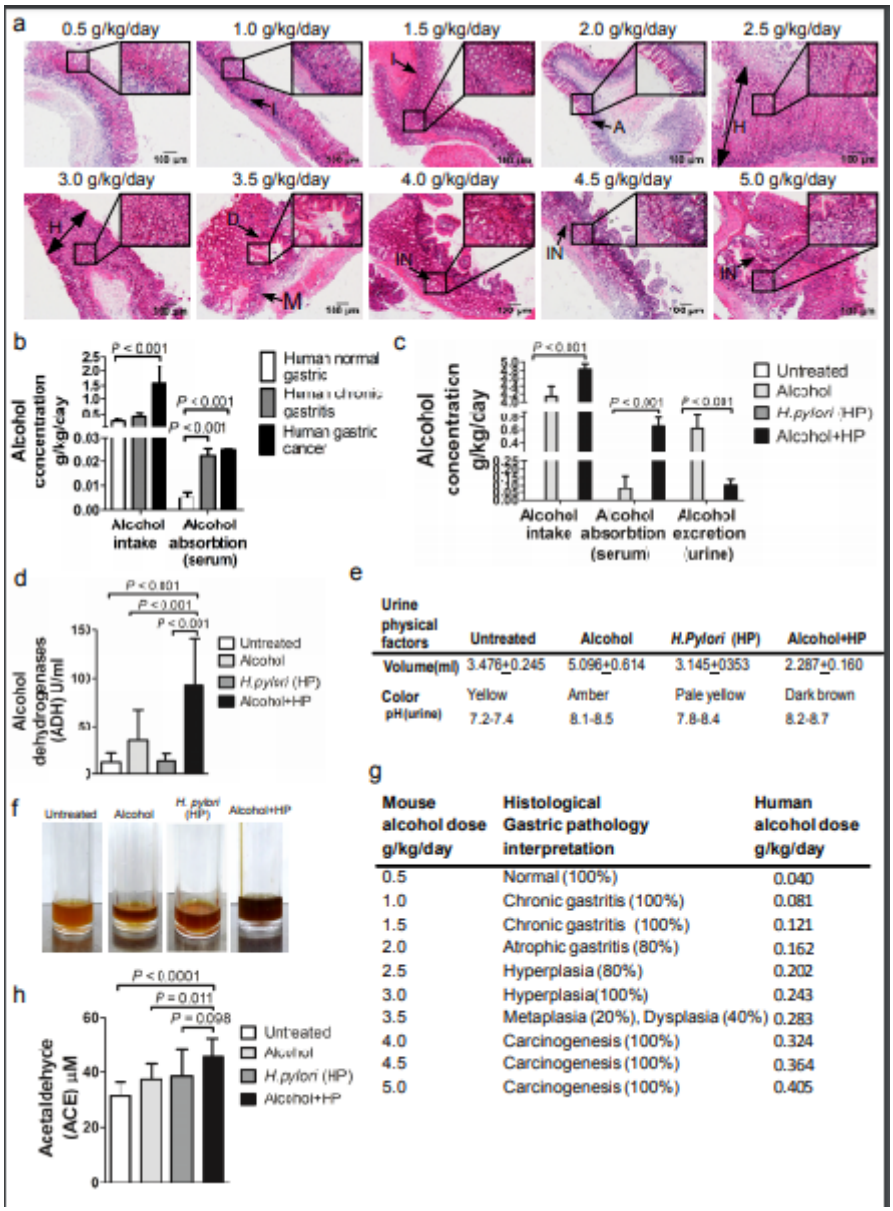

## Figure 2

Alcohol consumption in the development of gastric tumorigenesis. a) Dose-dependent response of alcohol intake on progression from gastritis to cancerous cell growth. The lowest dose (0.5 g/kg/day) of alcohol had no effect on gastric pathology compared to an intermediate dose (1.0-3.5 g/kg/day) or a higher dose (4.0-5.0 g/kg/day). Scale bars represent 100 μm (10x); the scale bar in the inset images represents 20 μm (40x magnification), (n = 5/cohort). Arrow and A= atrophy, H= hyperplasia, MT= metaplasia, I= inflammatory cells, IN= muscular mucosae invasion. Association of alcohol intake, metabolism, and excretion in mouse and human gastric disease samples. Alcohol concentration in b) human (n = 10) and c) mouse serum and urine samples was used to calculate alcohol intake, alcohol absorption (serum), and excretion (urine). d) Alcohol dehydrogenase (ADH) levels in mouse serum were measured. Mice exhibiting gastritis and tumorigenesis showed higher ADH biochemical activity compared to alcohol-only-treated or untreated mice. e) Analysis of urine samples from the gastric disease mouse models. Physical characteristics of mouse urine, including volume, color, and pH, were recorded for 35 days. f) Urine samples were collected and color differences were recorded from the different groups of mice. g) An equivalent dose of alcohol in mice and humans was determined by using a Km value of 3 (0.810). h) Acetaldehyde (ACE) levels in mouse urine were measured. Mice exhibiting gastritis and tumorigenesis showed higher acetaldehyde compared to alcohol-only-treated or untreated mice

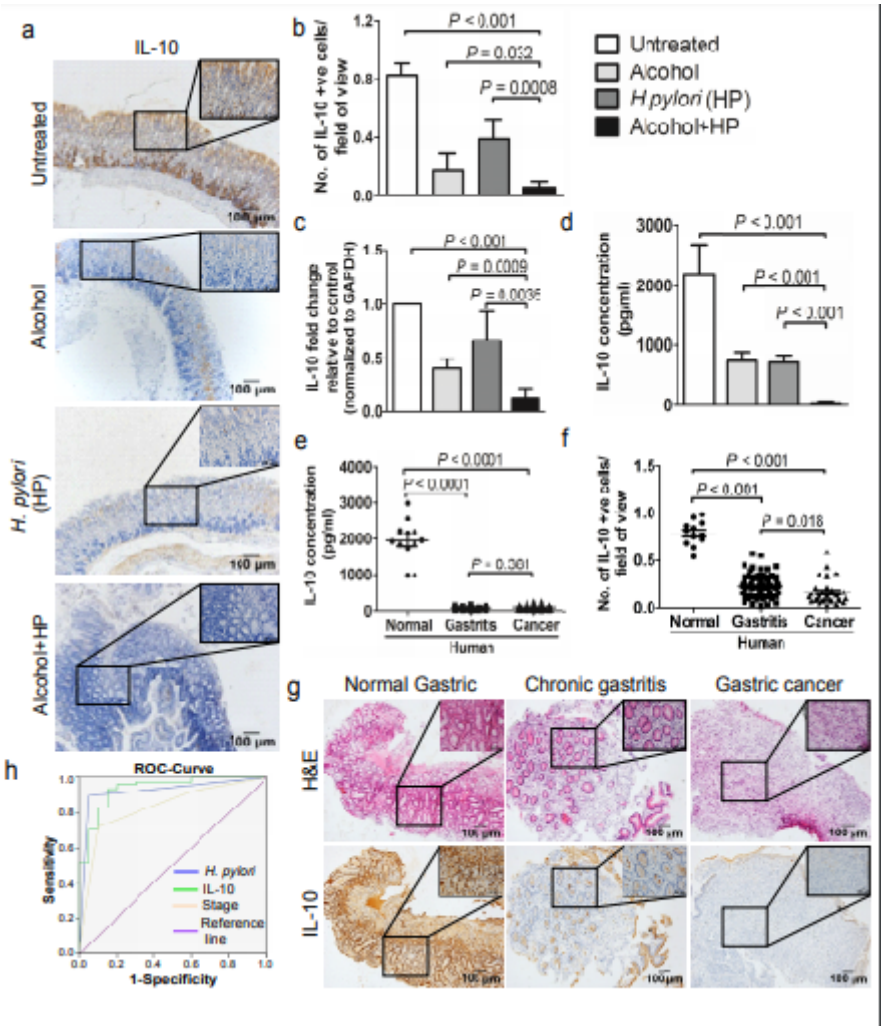

## Figure 3

Anti-inflammatory cytokine IL-10 expression in human gastric patients and mice treated with alcohol and infected with H. pylori. a) Immunohistochemical localization and b) histochemical analysis of IL-10 in tissue samples from mice treated with alcohol and infected with H. pylori (n = 5). c) qPCR mRNA analysis of IL-10 in mice exhibiting gastritis or gastric tumors. Bar graphs show average fold change in mRNA levels relative to untreated mice. d) IL-10 secretory protein levels in mouse serum samples were measured using a multiplex magnetic bead array. e) IL-10 protein secretion in healthy human subjects (n = 12) and in patients with gastritis (n = 35) or gastric cancer (n = 103) was measured using a multiplex magnetic bead array. f) Histochemical analysis and g) immunohistochemical localization of IL-10 in parallel human normal (n = 12), gastritis (n = 69), or gastric cancer patient mucosal tissues (n = 29). Scale bars represent 100 μm (10x), and the scale bar in inset images represents 20 μm (40x). h) ROC curve analysis to determine the association between alcohol consumption, H. pylori infection, and cancer in gastric cancer patients' serum samples. ROC curves are shown for each individual marker included in the classification algorithm, together with the clinical model and the H. pylori with alcohol consumption panel derived from logistic Lasso regression. Training set included 103 gastric cancer cases.

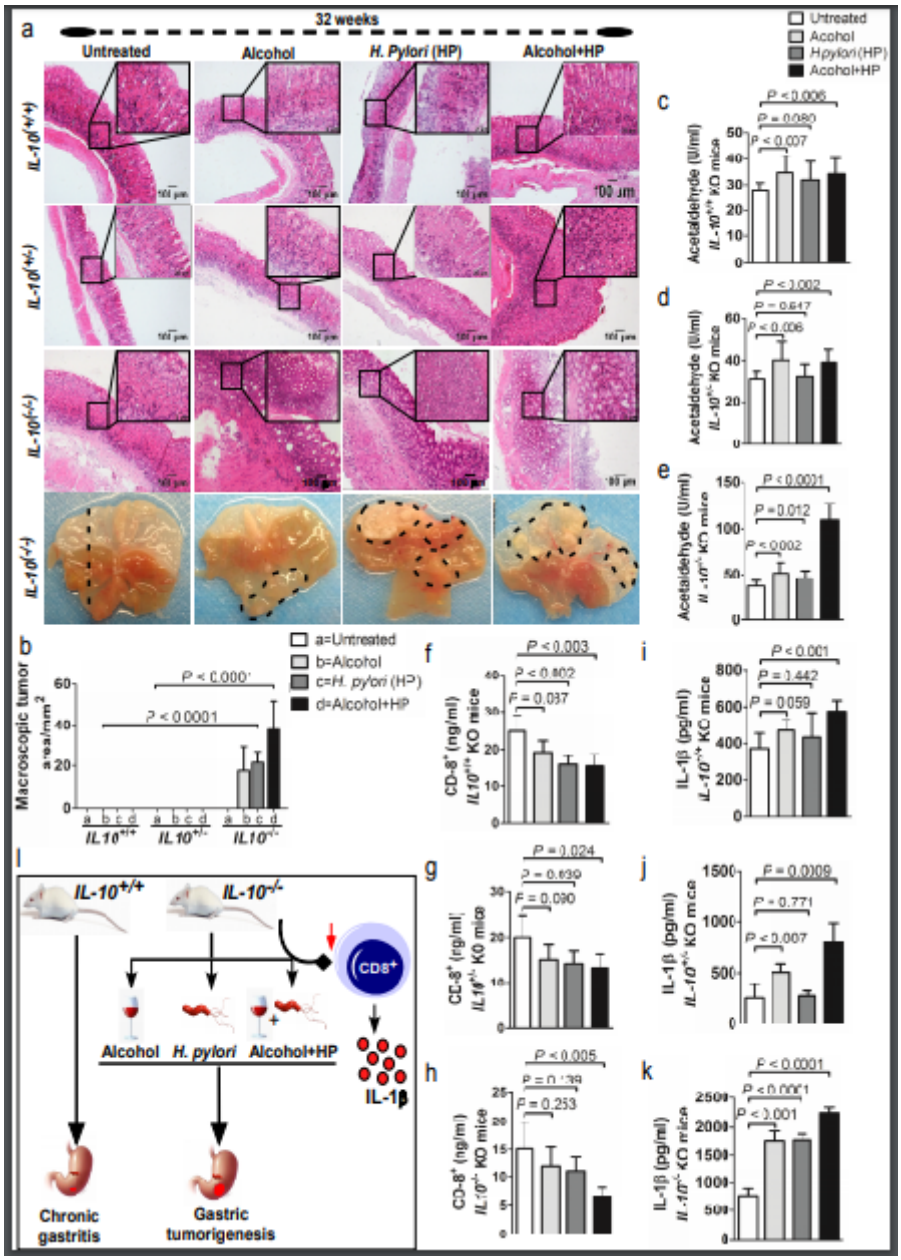


## Figure 4

IL-10 knockdown accelerates progression from gastritis to tumorigenesis in H. pylori-infected mice treated with alcohol. a) Histologic (top) and macroscopic (bottom) analyses of gastric mucosae in IL-10 knockout mice (n = 5/cohort). Hematoxylin and eosin (H&E) stained cross sections, cut along the fundus to the proximal end of the corpus as shown by straight dotted line. At 32 weeks, greater infiltration of inflammatory cells was observed in IL-10-/- mice with H. pylori infection. Tumors from H. pylori-infected mice treated with alcohol reveal severely disorganized dysplastic structures, extensive inflammatory cells recruitment, and epithelial destruction (32 weeks). Scale bars represent 100 µm (10x), and the scale bar in inset images represents 20 µm (40x). Tumor areas are outlined with dotted circles. b) Size of gastric tumors from IL-10-/- mice treated with alcohol and infected with H. pylori relative to tumor size from IL-10+/- and IL-10+/+ wild type mice. a) Untreated; b) alcohol-treated; c) H. pylori infected; d) gastritis induced by both alcohol and H. pylori; and e) tumorigenesis induced by both alcohol and H. pylori. (c-e)

Acetaldehyde levels in IL-10+/+, IL-10+/-, and IL-10-/- mice treated with alcohol or H. pylori. (f-h) Total level of CD8+ in IL-10+/+, IL-10+/-, and IL-10-/- mice treated with alcohol or H. pylori. (i-k) IL1β expression in IL-10+/+, IL-10+/-, and IL-10-/- mice treated with alcohol or H. pylori. l) Role of IL-10 mutation in the development and progression of gastric tumorigenesis.

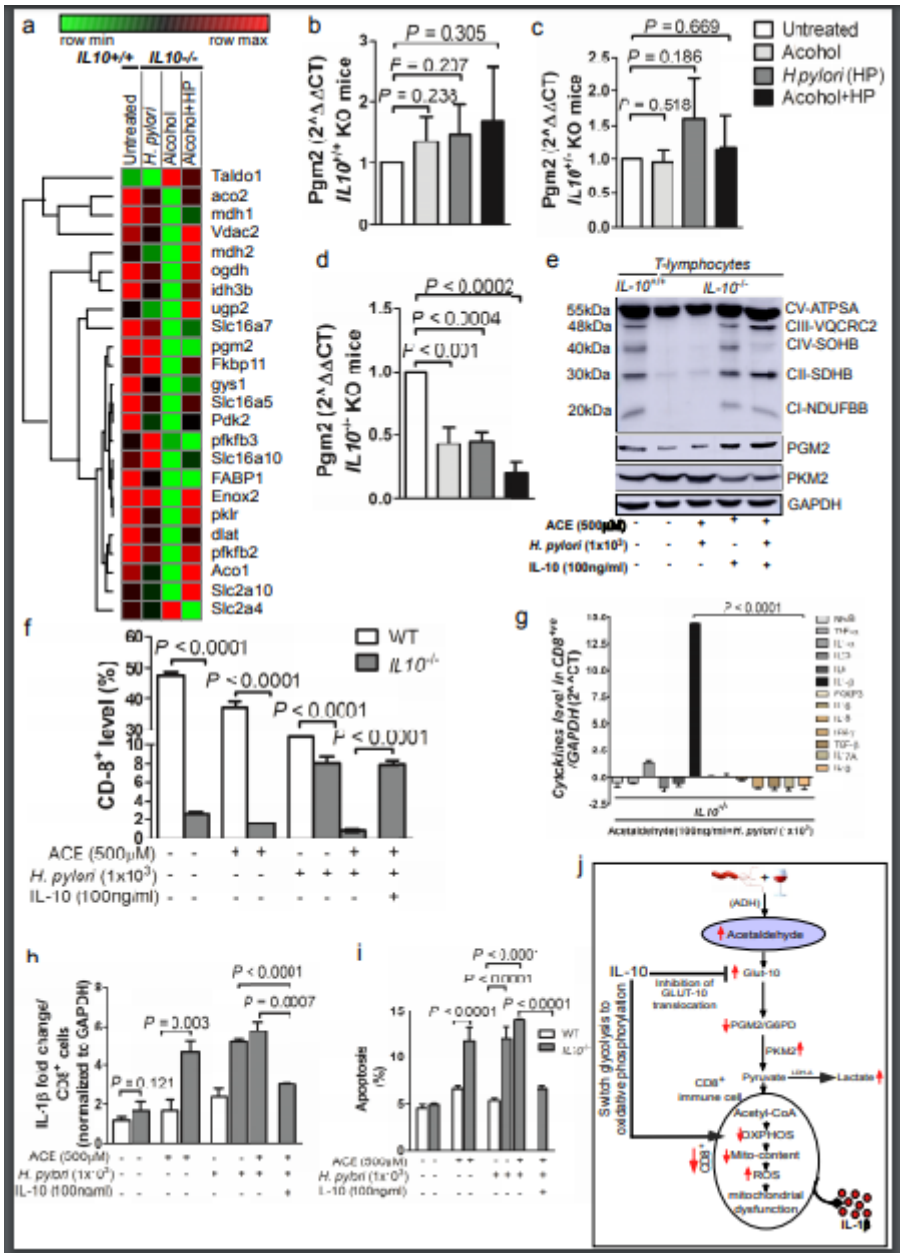


## Figure 5

IL-10 regulates glycolysis and mitochondrial function in CD8+ lymphocytes. (A) Heat map showing RNA-seq data, fold change of mitochondrial genes subset in IL-10+/+ and IL-10-/- mice treated with alcohol and H. pylori or alone. (b-d) Total mRNA expression of PGM2 in IL-10+/+, IL-10+/-, and IL-10-/- mice. (e) Oxidative phosphorylation and lactate production in WT or IL-10−/−-CD8+ cells measured via OXPHOS, PGM2, and PKM2 levels by Western blotting. (f) Relative CD-8+ immune cell percentages in wild-type (WT) or IL-10−/− mice stimulated with acetaldehyde (500uM) or H. pylori (1x103 cells/mL) in the absence or presence of IL-10 (100ng/mL) for 24h. (g) Cytokine profile of WT or IL-10−/−-CD8+ cells

measured by qPCR. h) Total mRNA expression of IL-1β in IL-10−/− CD8+ cells measured by qPCR i) Apoptosis level measured by Annexin-V-FITC assay in wild-type (WT) or IL-10-/- mice stimulated with acetaldehyde (500 μM) and/or H. pylori (1x103) in the absence or presence of IL-10 (100ng/mL) for 24h. j) Role of IL-10 mutation in mitochondrial dysfunction of CD8+ cells.

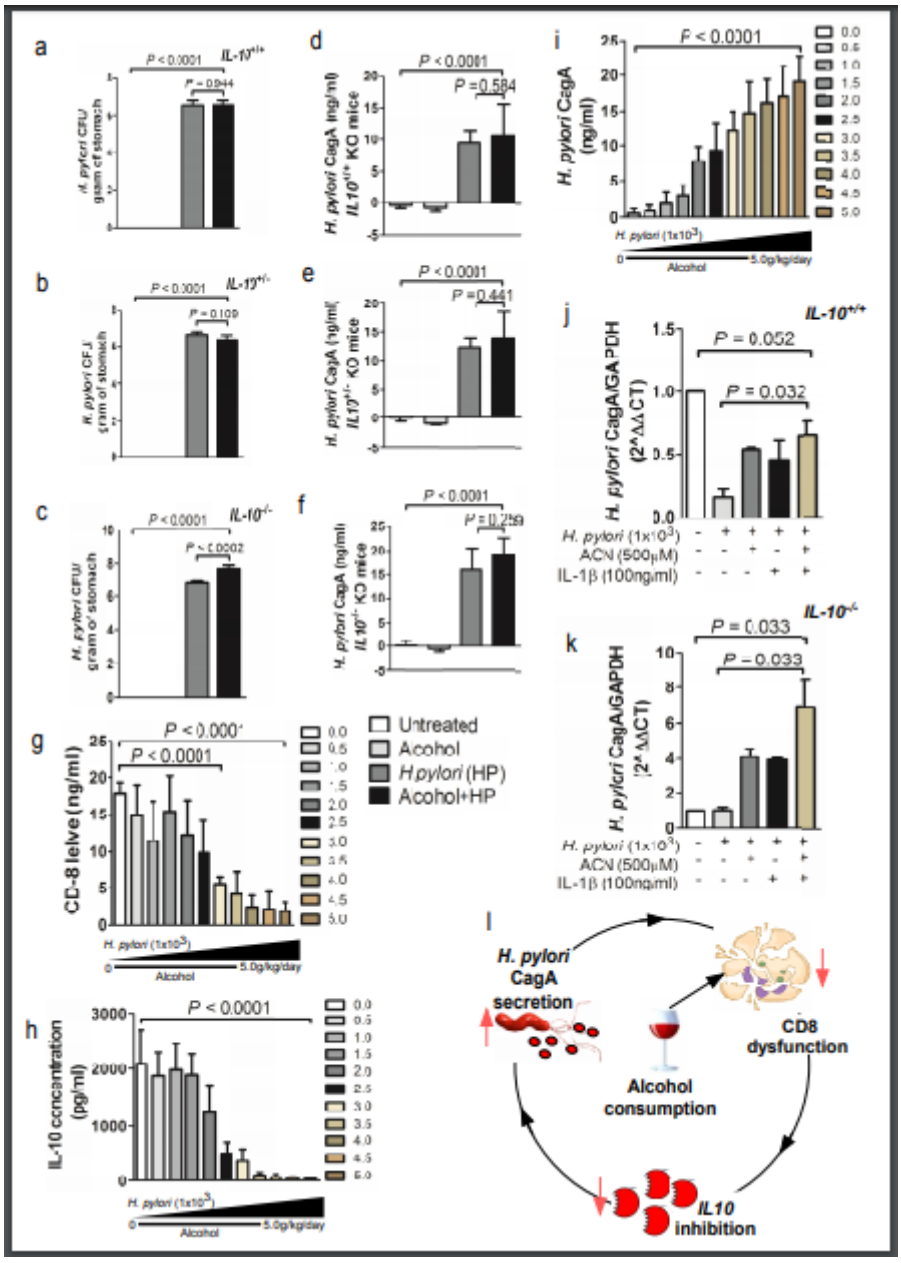


## Figure 6

Loss of IL-10 enhances H. pylori CagA infection due to lowered immunity upon alcohol intake. (a-c) Quantification of H. pylori (CFU/g of stomach) in IL-10+/+ and IL-10-/- mice treated separately or simultaneously with alcohol and H. pylori. (d-f) H. pylori CagA levels measured by ELISA in IL-10+/+ and IL-10-/- mice. (g-i) Dose-dependent response of alcohol intake on CD8 function, IL-10 production, and H pylori CagA infection as measured by ELSIA. (j-k) Quantification of H. pylori CagA using qPCR. Total mRNA expression of H. pylori CagA in wild-type (WT) or IL-10-/− mice stimulated with acetaldehyde

(500uM) or H. pylori (1x103) in the absence or presence of IL-1β (100ng/mL) for 24 h. (n = 5/cohort). l) Role of alcohol consumption in H. pylori infection due to CD8 cell dysfunction and IL-10 inhibition.

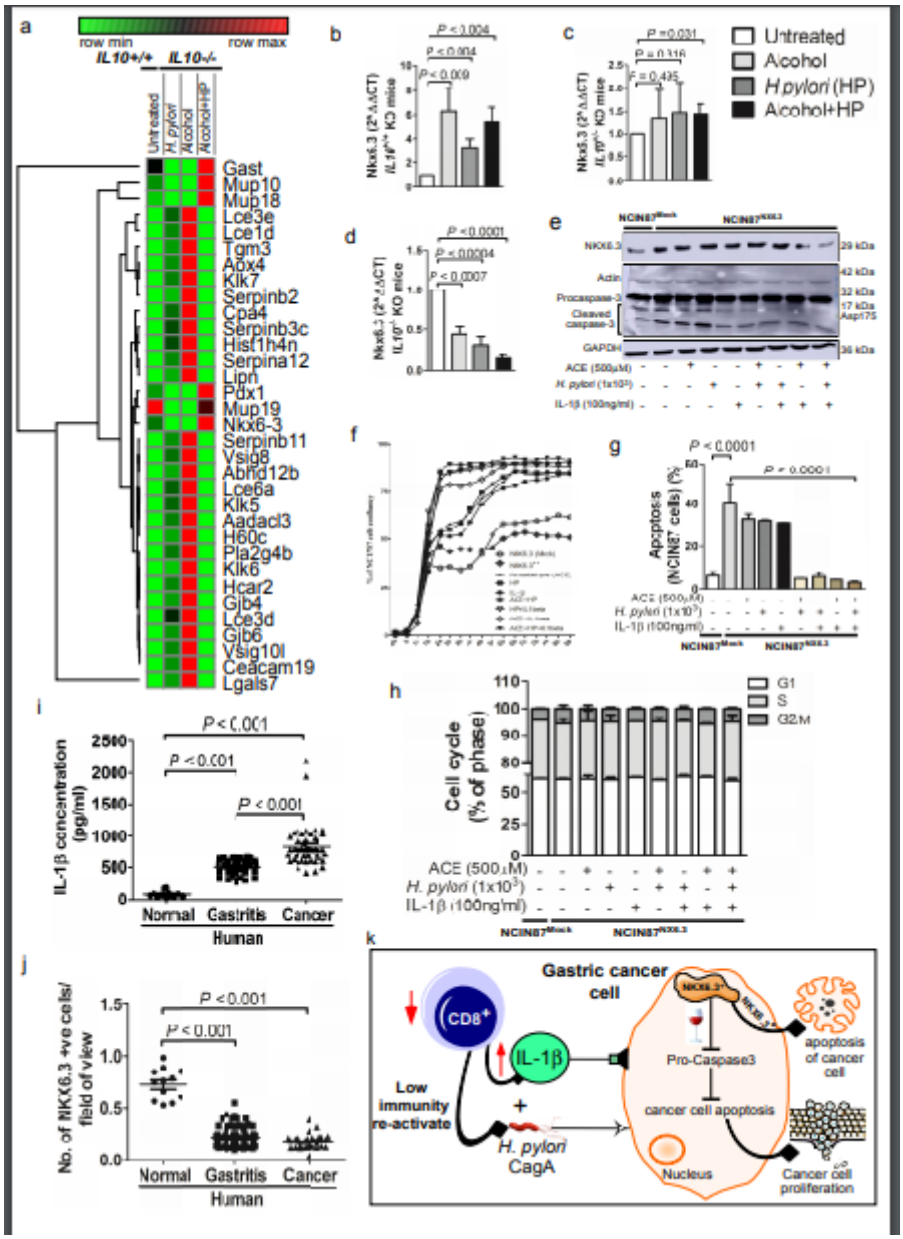


## Figure 7

IL-10 stimulates apoptosis of gastric cancer cells via NKX6.3 overexpression. (a) Heat map showing RNA-seq data, fold change of cancer gene subset in IL-10+/+ and IL-10-/- mice treated with alcohol and H. pylori or alone. (b-d) Total mRNA expression of NKX6.3 in IL-10+/+, IL-10+/-, and IL-10-/- mice treated with alcohol or H. pylori, (n = 5/cohort). (e) NKX6.3-associated-apoptosis in NKX6.3 overexpressed NCIN87 gastric cancer cells stimulated with acetaldehyde (500 μM), H. pylori (1x103) in the absence or presence of IL-1β (100ng/mL) for 24h, measured by caspase-3 levels via Western blotting. (f-h) Gastric cancer cell proliferation, apoptosis levels, and cell cycle progression measured by IncuCyteS3 imaging (Essen BioScience, serial number = IC50471), Annexin-V FITC staining, and propidium iodide staining, respectively. (i-j) beads array analysis and Immunohistochemical localization of IL-1β and NKX6.3 in

human normal (n = 12 & 12), gastritis (n = 36 & 69), or gastric cancer patient mucosal tissues (n = 45 & 29). Scale bars represent 100 μm (10x), and the scale bar in inset images represents 20 μm (40x). k) Effect of acetaldehyde treatment, H. pylori infection, and IL-1β production in the development and progression of gastric pathology mediated IL-10 inhibition.

## Supplementary Files

This is a list of supplementary files associated with this preprint. Click to download.

- SourceFile.xlsx
- Graphicalabstract.tif
- supplementaryfiguressmalllegends.pdf